


METHODS

Detecting *PKD1* variants in polycystic kidney disease patients by single-molecule long-read sequencing

Daniel M. Borràs^{1,2,3}  | Rolf H. A. M. Vossen⁴ | Michael Liem⁴ |
 Henk P. J. Buermans⁴ | Hans Dauwerse⁵ | Dave van Heusden⁵ | Ron T. Gansevoort^{6*} |
 Johan T. den Dunnen^{4,5,7} | Bart Janssen¹ | Dorien J. M. Peters^{5*} |
 Monique Losekoot^{7*} | Seyed Yahya Anvar^{4,5}

¹GenomeScan B.V, Leiden, The Netherlands

²Institut National de la Santé et de la Recherche Médicale (INSERM), Institut of Cardiovascular and Metabolic Disease, Toulouse, France

³Université Toulouse III Paul-Sabatier, Toulouse, France

⁴Leiden Genome Technology Center (LGTC), Department of Human Genetics, Leiden University Medical Center (LUMC), Leiden, The Netherlands

⁵Department of Human Genetics, Leiden University Medical Center (LUMC), Leiden, The Netherlands

⁶Department of Nephrology, University Hospital Groningen, University Medical Center Groningen, Groningen, The Netherlands

⁷Department of Clinical Genetics, Leiden University Medical Center (LUMC), Leiden, The Netherlands

Correspondence

Seyed Yahya Anvar, Department of Human Genetics, Leiden University Medical Center, Postzone: S-04-P, Postbus 9600, 2300 RC Leiden, the Netherlands.
 Email: s.y.anvar@lumc.nl

*On behalf of the DIPAK consortium.

Contract grant sponsor: European Union's Seventh Framework Programme FP7/2007-2013 (FP7-PEOPLE-2013-ITN-608332).

Communicated by Graham R. Taylor

Abstract

A genetic diagnosis of autosomal-dominant polycystic kidney disease (ADPKD) is challenging due to allelic heterogeneity, high GC content, and homology of the *PKD1* gene with six pseudogenes. Short-read next-generation sequencing approaches, such as whole-genome sequencing and whole-exome sequencing, often fail at reliably characterizing complex regions such as *PKD1*. However, long-read single-molecule sequencing has been shown to be an alternative strategy that could overcome *PKD1* complexities and discriminate between homologous regions of *PKD1* and its pseudogenes. In this study, we present the increased power of resolution for complex regions using long-read sequencing to characterize a cohort of 19 patients with ADPKD. Our approach provided high sensitivity in identifying *PKD1* pathogenic variants, diagnosing 94.7% of the patients. We show that reliable screening of ADPKD patients in a single test without interference of *PKD1* homologous sequences, commonly introduced by residual amplification of *PKD1* pseudogenes, by direct long-read sequencing is now possible. This strategy can be implemented in diagnostics and is highly suitable to sequence and resolve complex genomic regions that are of clinical relevance.

KEYWORDS

ADPKD, complex genomic regions, DNA diagnostics, long-read sequencing, PacBio, *PKD1*, single-molecule real-time sequencing, variant detection

1 | INTRODUCTION

DNA sequencing technologies have widely been applied in biomedical and biological research as well as diagnostics. Relatively low-cost and high-throughput are major advantages of next-generation sequencing (NGS) over standard diagnostic assays (Mardis, 2013; Oliver, Hart, & Klee, 2015; Su et al., 2011). However, despite widespread

use of NGS-based diagnostics strategies (Chang & Li, 2013; Codina-Solà et al., 2015; Dewey et al., 2014; LaDuca et al., 2014; Ligt et al., 2012; Ozsolak & Milos, 2011; Sun et al., 2015; von Kanel & Huber, 2013; Willig et al., 2015; Yang et al., 2013), short-read sequencing approaches such as whole-genome sequencing (WGS) and whole-exome sequencing (WES), often fail at reliably characterizing complex regions of the human genome (Chaisson et al.,

This is an open access article under the terms of the Creative Commons Attribution-NonCommercial-NoDerivs License, which permits use and distribution in any medium, provided the original work is properly cited, the use is non-commercial and no modifications or adaptations are made.

© 2017 The Authors. *Human Mutation* published by Wiley Periodicals, Inc.

2015; Lee & Schatz, 2012). These regions are often associated with extreme GC content, segmental duplications (SDs), low-complexity sequences, and gaps in the human reference sequence (Chaisson et al., 2015; Lee & Schatz, 2012; Steinberg et al., 2014). Single-molecule long-read sequencing can improve our understanding of genetic variations in complex but clinically relevant genomic regions (Guo et al., 2013; Laver et al., 2016; Loomis et al., 2013; Qiao et al., 2016).

In this study, we aim to show the value of single-molecule long-read sequencing as a tool to characterize genetic variants associated with autosomal-dominant polycystic kidney disease (ADPKD). ADPKD is a common inherited disease that accounts for 5%–10% of end-stage renal disease (Harris & Rossetti, 2010; Spithoven et al., 2014). Most ADPKD pathogenic variants occur in *PKD1* (MIM# 601313) and *PKD2* (MIM# 173910) genes with a reported prevalence of 85% and 15%, respectively (Barua et al., 2009; Harris & Rossetti, 2010). The mutation spectrums in *PKD1* and *PKD2* are highly heterogeneous, with no mutation hotspots present, indicating that pathogenic variants in either *PKD1* or *PKD2* are usually private (Gout, Martin, Brown, & Ravine, 2007; Harris & Rossetti, 2010). The screening of *PKD1* is challenging due to difficulties in amplification and low resolution of its complex locus (Qi et al., 2013; Rossetti et al., 2007; Tan et al., 2009). This is partly due to its high homology for most of *PKD1* sequence with six pseudogenes as well as high GC content (Qi et al., 2013; Rossetti et al., 2007; Tan et al., 2009). In this study, we used *PKD1* as an excellent example of a challenging and complex locus.

Several attempts have been made to improve the screening of *PKD1* gene by using short-read NGS approaches to replace the standard diagnostics based on Sanger sequencing and multiplex ligation-dependent probe amplification (MLPA) assays (Eisenberger et al., 2015; Mallawaarachchi et al., 2016; Qi et al., 2013; Rossetti et al., 2012; Tan et al., 2014; Trujillano et al., 2014). These strategies provided a clear diagnosis with high sensitivity and specificity (97%–100%) for 115 out of 183 (Rossetti et al., 2012), 16 out of 25 (Tan et al., 2014), 10 out of 12 (Trujillano et al., 2014), 35 out of 55 (Eisenberger et al., 2015), and 24 out of 28 (Mallawaarachchi et al., 2016) screened ADPKD patients. Duplicated and high GC content genomic regions, such as that of *PKD1* gene, can lead to ambiguous identification of variants when analyzed with short-read NGS strategies (Lee & Schatz, 2012). These ambiguities produced low true-positive variant detection rates of 28%–50% for the duplicated region of *PKD1* (Qi et al., 2013), and many false positives (10%) due to misalignments, low-quality alignments, and contamination by residual amplification of pseudogenes (Rossetti et al., 2012). Hence, diagnostic assays based on NGS short reads (e.g., Sanger or Illumina) may not be fully suited for reliable ADPKD diagnostics.

Here, we utilized the single-molecule long-read Pacific Biosciences RSII (PacBio) sequencing technology to assess its potential value in molecular diagnostics of ADPKD patients. We show that direct sequencing of long-range PCR (LR-PCR) products eliminates the interference of residual amplification of *PKD1* pseudogenes, as well as alignment ambiguities. This also enabled a reliable identification of pathogenic variants, from single-nucleotide variants (SNVs) to large deletions.

2 | MATERIALS AND METHODS

2.1 | Selection of subjects and DNA isolation

Nineteen genotyped patient samples were selected for this study from the diagnostic laboratory in which at least one pathogenic mutation was detected by Sanger sequencing or MLPA. The selection aimed to include different types of variants (e.g., SNVs, as well as small and larger insertions and deletions [indels]) that are located in exons or in immediately flanking intronic sequences, for both the duplicated regions as well as the unique part of *PKD1*. Although *PKD2* is not a complex gene and is not the focus of this study, the sequencing of LR-PCR fragments for *PKD2* was performed as a proof of principle of long-read sequencing and detection of variants also for *PKD2*. Genomic DNA isolation was performed from peripheral blood samples using PUREGENE nucleic acid purification chemistry on the AUTOPURE LS 98 Instrument (Qiagen).

2.2 | Long-read sequencing and variant identification for ADPKD genes

2.2.1 | LR-PCR amplification

To cover the entire *PKD1* and *PKD2* coding regions (including exon boundaries), a total of five and nine LR-PCR fragments were designed, respectively. Primers were optimized to produce amplicons of similar sizes (>4Kb) that could be pooled to improve sequencing efficiency and loading capacity for SMRT sequencing (Supp. Table S1; Supp. Fig. S1). The major part of *PKD1* intron 1 was excluded from the design due to its large size and the lack of previously reported pathogenic variants in this region. Fragments were amplified from 50 ng of genomic DNA using 1× Extensor Hi-Fidelity Long Range PCR Master Mix (Thermo Scientific, Massachusetts, USA) on a 25 μ l of PCR reaction volume with 200 nM of M13-tagged primers. Initial denaturation was performed for 10 min at 98°, followed by 35 cycles of 15 sec at 98° and 10 min at 68°, respectively. Final extension was 10 min at 68°. Products were size selected using the BluePippin DNA size selection system to classify them in three different groups of sizes 4.3–6.1, 7.1–7.5, and 7.6–8.1 Kb (Supp. Table S1; Supp. Fig. S1). Fragments of equal size were pooled equimolar, and were visually inspected by band intensity on agarose gel. Finally, all pools were purified with a 0.6× v/v ratio of AMPure XP Beads (Beckman-Coulter, Woerden, Netherlands).

2.2.2 | SMRT sequencing library preparation

Sample indexes for patient tracking were added to the LR-PCR fragments using an additional five-cycle PCR with the previous LR-PCR conditions. Barcoded pools were then purified with AMPure XP Beads, and pooled equimolar according to their size. Molar concentration was verified on a Bioanalyzer 12000 chip (Agilent, California, USA). For each barcoded pool, a SMRT-bell library was prepared according to the PacBio's 5- or 10-Kb Template Preparation procedures. Pooled amplicons were sequenced on five SMRT cells on the PacBio RSII system with the P6 sequencing chemistry. Data collected from 360-min movie time was preprocessed using the standard primary analysis tools (Fig. 1).

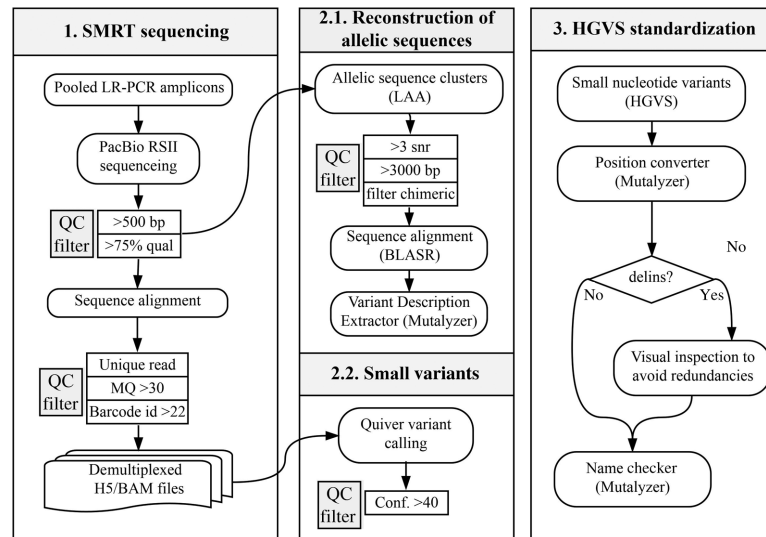


FIGURE 1 Flowchart of the applied analytical approach for the identification of potentially pathogenic variants and VUCS in ADPKD patient samples. Key processes in the workflow describe details and thresholds used for (1) sequencing of pooled LR-PCR amplified fragments with PacBio RSII and postprocessing of reads including alignments and read quality filters; (2) identification of variants using two independent strategies including the reconstruction of allelic sequences, and small variant calling using Quiver; (3) standardization of variant nomenclature to represent a correct HGVS description and facilitate the comparison between datasets; (4) enrichment of variant annotations with VEP (including effect prediction, ClinVar, SIFT, PolyPhen, 1000 Genomes Project, dbSNP, and SwissProt annotations among others), and selection of high-confidence variants; (5) identification of potentially pathogenic variants and VUCS based on their confidence, effect prediction, and population frequencies

2.2.3 | Sequence alignment and variant calling

We used the RS_Resequencing protocol from SMRT Analysis Suite v.2.3 to align long reads against the human reference genome, downloaded from the Genome Reference Consortium version 37 patch 13 (GRCh37.p13). Samples were demultiplexed into individual files (H5 and BAM formats) using known barcode sequences and a minimum barcode identity score of 22 (Fig. 1). Alignments were filtered to contain mapped reads with a mapping quality threshold of 30 Phred score using Samtools v.1.2 (Supp. Table S2). Read coverage and targeted PCR statistics for LR-PCR amplicons were computed with BedTools v.2.25.0, and PicardTools v.1.1.40 (Supp. Tables S2–S4). Variant calling was performed using Quiver (allowing for diploid calling and maximum coverage of 10,000). Variants with a Quiver confidence score lower than 40 were filtered out from downstream analysis (Fig. 1).

2.2.4 | Reconstruction of allelic sequences

PKD1 and *PKD2* allelic sequences were reconstructed using the Long Amplicon Analysis available in SMRT Analysis Suite 2.3. Only reads longer than 3,000 base pairs (bp) and average signal to noise ratio of three were used for the reconstruction (Fig. 1). Based on this reference-free subread (full-length and nonfull-length reads) clustering, chimeric sequences were identified and comprehended $\leq 0.85\%$ (6,288/738,822) of subreads that were subsequently removed from the analysis. Allelic sequences of *PKD1* and *PKD2* were aligned to the human reference genome GRCh37.p13 using BLASR (Chaisson & Tesler, 2012), and reporting a single best-scoring alignment. Variants were extracted by comparison between the reconstructed alleles and the human reference sequence with the Variant Description Extractor from the Mutalyzer Suite 2.0.21 (Vis, Vermaat, Taschner, Kok, & Laros, 2015).

2.2.5 | Loss of heterozygosity analysis

Loss of heterozygosity (LoH) for each amplified fragment was assessed to identify patients with potential large deletions for *PKD1*. We first identified heterozygous substitutions within the amplified fragments with a variant frequency between 25% and 75%. Amplified fragments with zero heterozygous substitutions were identified as LoH. Large deletions produce multiple LR-PCR fragments dropouts, and were identified by the detection of consecutive LoH fragments. The detection of consecutive LoH fragments was not a direct identification of large deletions per se, rather than an indication of the presence of large deletions in the amplified LR-PCR fragment regions. Identified LoH regions were then compared with large deletions detected by MLPA.

3 | ADPKD VARIANT NOMENCLATURE AND GENOTYPING

Variant descriptions were standardized to concord with HGVS guidelines (den Dunnen et al., 2016), using the Mutalyzer Name Checker tool (Wildeman, van Ophuizen, Dunnen, & Taschner, 2008). Genomic HGVS descriptions were converted to coding notations using the Position Converter from Mutalyzer (Wildeman et al., 2008). Only changes in RefSeq-annotated canonical transcripts for *PKD1* (NM_001009944.2) and *PKD2* (NM_000297.3) were further analyzed. HGVS descriptions of deletion–insertions (delins) were manually inspected to avoid variant redundancies and undesired clustering of neighboring independent events (Fig. 1; Supp. Table S5). Then, standardized variants were annotated using the Variant Effect Predictor (VEP), from Ensembl tools v.83 (McLaren et al., 2010), with additional parameters “-everything,” and “-refseq” (Fig. 1). All variant annotations reported by VEP are fully disclosed in the raw VCF files (EGAS00001002106). Variant frequency

and coverage were used to filter low-confidence variants by applying thresholds for: (1) sequencing depth of $\geq 50\times$ subreads and $\geq 15\times$ reads that ensures a sufficient control over the SMRT sequencing random error rate (1% mismatches and 13% indels) and (2) minimum variant frequency of 10% for substitutions and 15% for delins (Fig. 1). For interpreting insertion and deletion frequencies, neighboring bases were also examined. The selection of strong pathogenic variant candidates or variants of unknown clinical significance (VUCS) was based on the following criteria: (1) high predicted effect on the coding sequence or splice-site region (e.g., missense, in-frame indels, frameshifts, and splice-site acceptor or donor variants); (2) population frequency in the 1000 genomes project $< 1\%$; (3) unique occurrence (1/19) ($\sim 5\%$) in the patient cohort since, in ADPKD, no single disease-causing variant accounts for more than 2% of affected families (Harris & Rossetti, 2010), or more than 1.7% of ADPKD reported cases in the ADPKD database (PKDB) (<http://pkdb.mayo.edu/>; accessed version 3.1) (Gout et al., 2007) (Fig. 1).

3.1 | Clinical diagnostics pipeline for ADPKD genotyping

3.1.1 | Sanger sequencing

The current diagnostics pipeline for ADPKD genotyping, including Sanger sequencing and MLPA, uses a different set of LR-PCR primers to target the duplicated part of *PKD1* (exons 1–32) (Supp. Table S6). The nonduplicated region of *PKD1* (exons 33–46), and *PKD2* regions (exons 1–5) were amplified using targeted standard PCR reactions (Supp. Fig. S1), with 100 ng of input genomic DNA with M13 tail primers. The nested and standard PCR amplicons were designed to cover the complete coding regions and splice sites with at least 20 bp of flanking intronic sequences (Supp. Tables S7 and S8). The duplicated part of *PKD1*, which includes exons 1–32, was amplified using four different LR-PCR fragments that covered exons 1, 2–13, 14–21, and 22–32, respectively (Supp. Table S6). LR-PCR amplification was performed using Thermo Scientific (Massachusetts, USA) 2 \times Extensor Long Range PCR Master Mix on 50 ng of DNA. Then, a nested PCR was carried out on 4 μ l 100–250 \times of diluted product to obtain the final Sanger sequencing fragments. The nested PCR primers with an M13 tail were used to amplify the coding region including 5–20 bp of intronic sequences (Supp. Fig. S1). Large exons such as exon 5, 10, 11, 15, and 23 were amplified using overlapping nested PCR products, although 10 bases of exon 15 (c.6503–6514) were not covered. Nested PCR and standard PCR of the nonduplicated part of *PKD1*, and *PKD2*, was carried out in a final volume of 15 μ l in GoTaq Colorless Taq Reaction buffer with 0.6 U of Taq DNA polymerase (Promega, Leiden, Netherlands) at a final concentration 5 pM for each primer, 200 μ M of each dNTP. After a hot start at 95°C, a denaturation was performed for 5 min at 95°C, followed by 35 cycles of 45 sec at 94°C, 45 sec at 60°C, and 30 sec at 72°C. The final extension was of 5 min at 72°C in a T-Professional Thermocycler (Biometra, Göttingen, Germany; Westburg, Leusden, Netherlands). All liquid handling steps were automated using the SciClone (ALH-HV96 pipetting station; Perkin Elmer, Massachusetts, USA) or Biomek FX workstation (Beckman-Coulter, Woerden, Netherlands). PCR products (20–50 ng) were purified using an

Ampure XP PCR purification kit and sequenced using BigDye Terminator v3.1 sequencing reactions (Applied Biosystems, California, USA) with PAGE purified –21M13 or M13REV sequencing primer. The excess of dye terminations was removed by gel filtration using the Edge Biosystem Dye Terminator Removal (DTR) with a 96-well plate. After electrophoresis on an ABI Prism 3730 (XL) DNA analyzer (Life technologies, California, USA; Applied Biosystems, California, USA), data processing was automated using SeqPatient software (Sequence Pilot, JSI Medical Systems GmbH, Ettenheim, Germany).

3.1.2 | MLPA

To detect large deletions and duplications, two commercially available MLPA kits (P351-B2 and P352-C1; MRC-Holland, Amsterdam, The Netherlands) were used following manufacturer's protocols and manuals.

3.2 | Comparative analysis of SMRT sequencing and current ADPKD diagnostic assay

The overlap between identified variants based on PacBio and Sanger sequencing data was achieved by assessing identical standardized HGVS descriptions. Only variants with predicted effects on coding DNA or splice-site regions were considered (Supp. Table S5). PacBio and Sanger variants were manually inspected to detect overlapping variants with discordant descriptions between the two datasets. To facilitate interpretation, each unique variant was further annotated with its PKDB clinical significance, single-nucleotide polymorphism database version 144 (dbSNP) identifier, and the number of patients where it was detected in the cohort. Surrounding bases were evaluated to identify and remove potential sequencing artifacts occurring in homopolymer stretches. Finally, variants were considered as high-confident variants if previously reported in PKDB or dbSNP, showed strong PacBio sequencing evidence of being present, or detected in any patient by both Sanger and PacBio sequencing.

3.3 | Short-read loss of power for known *PKD1* pathogenic variants in WGS and WES

Previously known pathogenic variants for *PKD1* gene were obtained from PKDB. Only variants that were classified as “definitely pathogenic” were selected for further analysis. Large deletions (few hundred bp to several Kbp long) were excluded from the analysis as they are not usually detected with common variant calling algorithms. For the genomic position of each pathogenic variant, sequencing depth was extracted from nine publicly available WGS and WES datasets (Sun et al., 2015). In addition, we included the sequencing depth of nine randomly selected libraries from the study of Rossetti et al. (2012), in which the authors used a similar strategy based on LR-PCR and followed by short-read sequencing. Each library represents an equimolar pool of DNA from four different patient samples that were not possible to further demultiplex because individuals were not barcoded. Variant positions with low sequencing depth (< 8 reads, or < 32 for the short-read LR-PCR approach) were marked as inaccessible positions of clinical significance using BedTools v2.25.0. Finally, variant positions were classified into three categories based

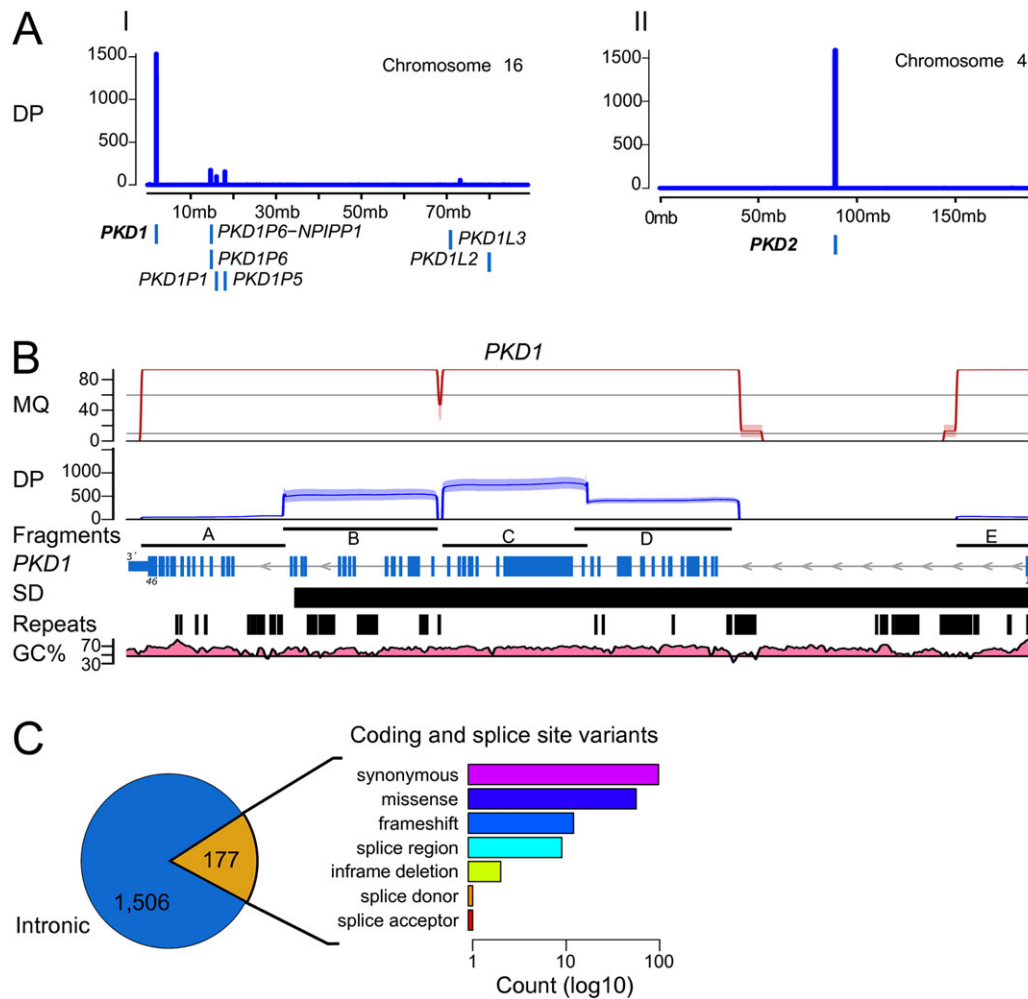


FIGURE 2 SMRT sequencing and variant calling of LR-PCR amplicons. **A:** Sequencing depth (DP; in number of reads) of the alignments to chromosome 16 and chromosome 4. Number of uniquely aligned reads (y axis, blue line) sequenced with PacBio that mapped to *PKD1* and *PKD2*. Off-target amplification is discriminated from the main *PKD1* gene sequences showing alignments to pseudogene homologous sequences at proximal loci (e.g., *PKD1P1*, *PKD1P5*, *PKD1P6*) (blue boxes). **B:** Mapping quality (MQ; in Phred quality scores; values >90 were scaled down for visualization purposes), and sequencing depth (DP; in number of reads) of uniquely aligned molecules to *PKD1* (NM_001009944.2) for the five LR-PCR fragments amplified. Mapping quality of alignments with even coverage distribution along the amplified fragments (fragments), including regions with SDs, repetitive elements (repeats), and high GC content (GC%). Despite fragments A and E showing lower coverage, compared with the average sequencing depth of $\geq 421\times$ (minimum $\geq 19\times$; maximum 1,528 \times), they had sufficient coverage for variant calling within the exon regions, including the first exons of *PKD1*, with average coverage of $\geq 55\times$ (minimum $\geq 24\times$; maximum 91 \times) (Supp. Table S4). **C:** We detected 1,506 intron variants (blue) and 177 coding or splice-site variants (yellow). The predicted transcript effects of coding and splice-site variants were quantified (bar chart) as log₁₀ count (x axis)

on the number of individuals with poor coverage at each position: (1) variants with sufficient coverage in all nine individuals; (2) variants reported inaccessible in two to four individuals; and (3) variants reported inaccessible in five or more individuals.

3.4 | Data availability

Sequencing data and alignments in BAM format can be accessed through the European Genome-phenome Archive (EGA), as well as raw variants in VCF file format, under the EGA study identifier EGAS00001002106. Coding or splice-site variants were also uploaded to the Leiden Open Variation Database (LOVD). Description and examples of custom scripts used in this manuscript are accessible upon request from a local GitLab repository.

4 | RESULTS

4.1 | Targeted sequencing of ADPKD genes

Direct sequencing of LR-PCR fragments (designed to specifically and uniquely amplify *PKD1*, and *PKD2* gene regions) (Supp. Fig. S1; Supp. Table S1) was performed to evaluate the utility of long-read sequencing in resolving ADPKD for molecular diagnostics. All *PKD1* and *PKD2* exons (including the duplicated part of *PKD1*, as well as 20 bp of flanking intron regions) from 19 ADPKD patients could be completely covered using long reads, sequenced on the PacBio RSII platform (Fig. 2; Supp. Fig. S2). Most of the long reads (94.4%) were uniquely mapped to *PKD1* and *PKD2* (Supp. Table S2). Reads originating from residual off-target amplification (5.6%; Supp. Table S2) introduced during the

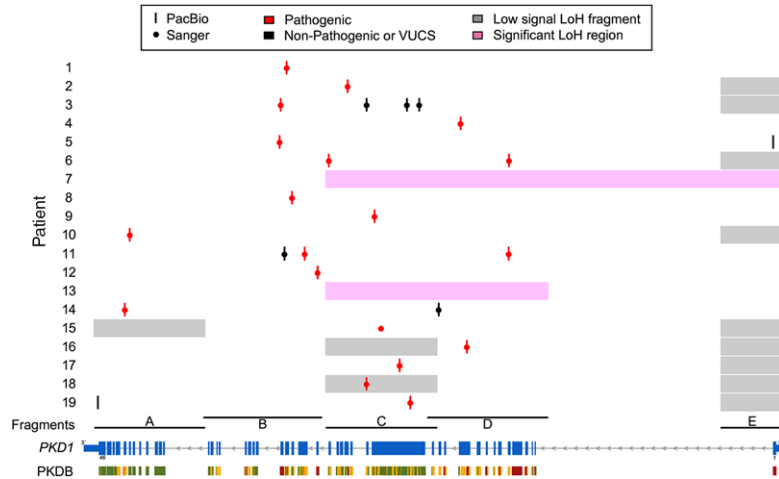


FIGURE 3 Comparison of long-read detected pathogenic variants or VUCS, uniquely identified per patient (y axis), with the screening results for the *PKD1* gene locus (x axis; NM_001009944.2). Most of the pathogenic variants (red) could be confirmed by our long-read strategy (red bars) with high sensitivity for *PKD1*. Only a single insertion could not be confirmed for patient 16. Other identified nonpathogenic variants or VUCS are shown as black bars and dots for PacBio and Sanger, respectively. The LoH analysis performed (pink or gray boxes) support the presence of the two large deletions also reported by MLPA (pink boxes). LoH regions are not a direct identification of large deletions but a clear indication of their presence within the amplified LR-PCR fragments

LR-PCR steps were identified, and discriminated, by their unique alignment to the *PKD1* pseudogenes (Fig. 2; Supp. Table S2). All *PKD1* and *PKD2* protein coding and flanking intron sequences (± 20 bp) were covered at average sequencing depth $\geq 421\times$ (minimum $\geq 19\times$; maximum 1,528 \times), with $\geq 97.36\%$ of bases over $\geq 30\times$, which was well above the applied threshold of $\geq 15\times$ reads (Supp. Tables S2 and S4). Amplicons that cover the first and last exons of *PKD1* were underrepresented when compared with other LR-PCR fragments, with a total of ≥ 593 average reads (minimum ≥ 300 ; maximum 1,580) and ≥ 87 (minimum ≥ 35 ; maximum 153) for *PKD1* fragments A and E, respectively (Fig. 2B; Supp. Table S3). The usually difficult to sequence first exons of both *PKD1* and *PKD2* genes were covered, on average $\geq 55\times$ (minimum $\geq 24\times$; maximum 91 \times) and $\geq 71\times$ (minimum $\geq 43\times$; maximum 111 \times), respectively (Supp. Table S4). Most of the sequenced reads ($>99.9\%$) were uniquely mapped to *PKD1* and *PKD2* (Fig. 2B; Supp. Fig. S2).

4.2 | Sensitive detection of ADPKD small variants

PKD1 is known to be a highly polymorphic gene with many variants reported in addition to the disease-causing or pathogenic variants (Gout et al., 2007). Hence, the required sensitivity to resolve *PKD1* was achieved by the combination of variant calling using Quiver and the reconstruction of amplified allelic sequences. Overall, we identified 1,683 variants (404 SNVs) across 19 ADPKD patients, from which 177 variants (119 SNVs) were located in coding or splice-site regions (Fig. 2C). Variants were distributed along *PKD1* (Supp. Fig. S3A) including regions with large SDs and high GC content. The mismatch rate of PacBio data was empirically assessed based on average frequency of mismatches at each position. We observed an average of 1.2% mismatch rate across the entire *PKD1* gene (Supp. Fig. S3A). This correlates with the random sequencing mismatch rate of 1% for PacBio, and thus the applied minimum frequency threshold of 10% for substitu-

tions is well above the observed noise introduced by random PacBio errors.

4.3 | Large deletions in *PKD1*

Detection of allele dropouts and large deletions in *PKD1* was assessed by performing a LoH analysis for each of the amplified regions (Fig. 3). We identified 17 LR-PCR fragments with LoH among all 19 patients sequenced. Most of LoH regions (10) were identified in fragment E (Fig. 3). Only two patients showed consecutive LoH fragments indicating the presence of large deletions spanning between two or more LR-PCR fragments. These consecutive LoH fragments are not a direct identification of the deletions per se but an indication of the presence of large deletions in the amplified region. The two patients that showed two or more consecutive fragments with LoH (Fig. 3) were in concordance with large deletions identified by MLPA as pathogenic variants in the same ADPKD patients. A deletion of $\geq 1,543$ bp (c.(2097+1_2098-1)_3640del; exons 11–15) and a deletion of $\geq 9,108$ bp (c.(287+1_288-1)_(9397+1_9398-1)del; exons 3–26) were detected by MLPA for patient sample 7 and 13, respectively. With the current experimental design, however, the exact location of the breakpoints for each large deletion could not be determined with either method.

4.4 | Comparative analysis between SMRT-Seq and the ADPKD diagnostic assay

The evaluation of 167 coding or splice-site variants identified by standard ADPKD diagnostic assay showed that 159 out of 167 were correctly detected by PacBio (Supp. Fig. S3C). The overall observed sensitivity and specificity in detecting coding variants was of 95.2% (159/167) and 88.8% (159/179), respectively. Eight variants were

solely detected by Sanger (Supp. Fig. S3A: crosses), from which, despite the high sequencing depth, the majority (6/8) had low number of reads supporting the presence of these variants in PacBio sequencing data with variant frequency below the applied frequency thresholds (Supp. Fig. S3B: yellow dots). The remaining 2/8 variants (Supp. Fig. S3B: red dots) constitute a pathogenic insertion (c.6223_6224insTT) and one polymorphic substitution (c.12630T > C) (Supp. Table S9; Supp. Fig. S4).

From 179 variants detected by PacBio, 20 were solely identified by PacBio (Supp. Fig. S3C; Supp. Table S9). Of these, 17/20 were high-confidence variants not detected in Sanger. The remaining 3/20 were low-confidence variants from the reconstruction of allelic sequences for the variant c.6657_6671del (Supp. Table S9).

The sensitivity assessment for *PKD1* pathogenic variants was performed by comparing the list of potentially pathogenic variants and VUCS, uniquely identified by our direct long-read sequencing approach, with the results from the standard ADPKD diagnostic assay. Although we expected a single dominant pathogenic variant per patient, two of the patients had a combination of two pathogenic variants resulting in 21 *PKD1* pathogenic variants. We identified 20 out of 21 pathogenic variants (95.2%) in addition to seven VUCS from which two were uniquely detected by PacBio (Table 1; Fig. 3). Only a single pathogenic insertion (c.6223_6224insTT) was missed by PacBio variant calling despite sufficient read support (43.3% variant frequency; read depth 1,203) (Table 1). In summary, 18 out of 19 ADPKD patients could be resolved by our method (Fig. 3). This provided a diagnosis for 94.7% of the patients, resulting in the correct detection of all *PKD1* substitutions, single-nucleotide deletions, large deletions, one delin, and three out of four insertions or duplications (Table 1).

4.5 | Loss of *PKD1* diagnostic power in short-read (Illumina) NGS

The potential loss of diagnostic power when resolving *PKD1* by short-read NGS was evaluated based on 797 pathogenic variants that were previously reported and validated, and are publicly available in PKDB. The repetitive nature of *PKD1* gene hampers proper alignment of short Illumina NGS reads (Supp. Fig. S5). Over 12% of the reported pathogenic variants would have been missed in WGS and WES data purely due to poor sequencing depth (Supp. Fig. S6). In comparison, other short-read approaches based on LR-PCR enrichment show lower percentage (1.3%) of reported pathogenic variants that would have been missed because of low sequencing depth. However, this approach required very high sequencing depth, which can be appreciated from the observed high variability in coverage ranging from <8× to >30,000× (Supp. Fig. S6). Moreover, several exonic regions may be expected to be missed in many samples, irrespective of the short-read sequencing strategy used (Supp. Fig. S6).

5 | DISCUSSION

Accurate diagnosis is a difficult task when performed in complex genetic regions such as *PKD1* (Qi et al., 2013; Rossetti et al., 2007; Tan et al., 2009). To facilitate the diagnosis, we have developed and applied

a new methodology using direct long-read sequencing of amplified LR-PCR fragments on PacBio. Because of the repetitive nature of *PKD1*, current diagnostics is performed by Sanger sequencing using LR-PCR fragments generated for approximately two thirds of the *PKD1* gene that serve as a template for the exon-specific nested PCR amplification. In contrast, in this study, we directly sequenced all LR-PCR fragments amplified from the duplicated and unique parts of *PKD1* gene as well as *PKD2*. On top of reducing the PCR amplification steps required and limiting the implicit PCR artifacts, single-molecule sequencing improves sequence alignments and aids in discriminating between homologous or repeated sequences, such as *PKD1* pseudogenes. This provides a cleaner dataset for variant calling, free of chimeric (0.85%) and pseudogene (5.6%; Supp. Table S2) reads that are introduced by the LR-PCR amplification. Finally, by using this approach, we identified 20 out of 21 (95.2%) *PKD1* disease-causing variants diagnosed by Sanger sequencing or MLPA, providing a correct diagnosis for 18 out of 19 ADPKD patients (94.7%) with at least one pathogenic variant in *PKD1*.

In comparison to current ADPKD diagnostic assays, based on Sanger sequencing and MLPA, we show that direct long-read sequencing can aid in resolving *PKD1* for ADPKD diagnostics. Longer sequencing reads discriminate between *PKD1* and pseudogenes (Fig. 2A), and improve the mapping quality of *PKD1* (Fig. 2B). The improved mappability reduced the interference of homologous sequences, high GC content, or repetitive elements for ADPKD diagnosis (Qi et al., 2013). This allowed us to develop a long-read-based sequencing assay for detecting a broad spectrum of variants, from SNVs to large deletions (Table 1). In contrast, Sanger sequencing is very labor-intensive and requires many phases of overlapping PCR amplification steps prior to sequencing, including LR-PCR and nested PCR. Despite the amplification of *PKD1* being based on unique PCR primers, these are of limited number for *PKD1* and have been shown to produce residual amplification of homologous regions that would still interfere with the aggregated signal of Sanger sequencing (Rossetti et al., 2012; Tan et al., 2014). Based on our approach, we confirmed the presence of residual amplification of *PKD1* pseudogenes, introduced by the LR-PCR (5.6%) (Fig. 2A; Supp. Table S2). This, most likely, led to the identification of 24 false-positive or false-negative variants detected by Sanger sequencing (Supp. Table S9; Supp. Fig. S4). One of the major drawbacks of our method, however, is the noise associated with PacBio sequencing, and the sophisticated algorithms required to overcome it. This noise is likely to be the cause of most of the 324 homopolymer deletion artifacts that were solely identified by PacBio (Supp. Table S10). In addition, this noise was the most likely cause of the single pathogenic insertion that was missed despite ample sequencing depth. However, based on a recent release of the new circular consensus calling algorithm for PacBio sequencing data (www.pacb.com: "An improved circular consensus algorithm with an application to detect HIV-1 drug-resistance associated with mutations (DRAMS)"), we expect that calling of true homopolymer-associated variants will be significantly improved.

In recent years, several attempts have been made to replace the standard ADPKD diagnostics by NGS approaches that would improve the screening of *PKD1* gene (Eisenberger et al., 2015; Mallawaarachchi et al., 2016; Qi et al., 2013; Rossetti et al., 2012; Tan et al., 2014; Trujillano et al., 2014). These screenings were based on

TABLE 1 Uniquely identified pathogenic variants or variants of unknown clinical significance identified by PacBio sequencing

Patient	Genomic position	Exon	c. notation	p. notation	SNP ID	Freq (%)	Depth	PolyPhen	VEP impact	Comparison with Sanger sequencing
1	chr16 2,152,543	25	c.9034_9039del	p.(Thr3012_Ser3013del)		40.9	314		Moderate	Overlap
2	chr16 2,156,674	18	c.7214G > T	p.(Trp2405Leu)		29.4	666	Probably damaging (0.983)	Moderate	Overlap
3	chr16 2,161,525	15	c.3643C > G	p.(Leu1215Val)	rs144338515	49.2	576	Possibly damaging (0.899)	Moderate	Overlap
3	chr16 2,160,693	15	c.4475G > C	p.(Arg1492Pro)	rs575211353	32.8	563	Possibly damaging (0.665)	Moderate	Overlap
3	chr16 2,157,963	16	c.6986G > A	p.(Arg2329Gln)	rs780284643	43.3	538	Benign (0.37)	Moderate	Overlap
3	chr16 2,152,134	26	c.9324del	p.(Ile3109SerfsTer207)	rs780284643	26	302		High	Overlap
4	chr16 2,164,333	11	c.2681_2690del	p.(Phe894Ter)		53.7	143		High	Overlap
5	chr16 2,185,509	1	c.182C > T	p.(Pro61Leu)		28.8	43	Benign (0.119)	Moderate	PacBio
5	chr16 2,152,061	26	c.9397 + 1G > A			23.3	330		High	Overlap
6	chr16 2,167,614	6	c.1261C > T	p.(Arg421Cys)		38.7	273	Possibly damaging (0.836)	Moderate	Overlap
6	chr16 2,155,399	21	c.7940C > T	p.(Thr2647Met)	rs748496650	44	357	Probably damaging (1)	Moderate	Overlap
7	chr16 2,161,527		c.(2097 + 1_2098-1)_3640del							PacBio
8	chr16 2,152,903	24	c.8859dup	p.(Glu2954Ter)		44.1	583		High	Overlap
9	chr16 2,158,496	15	c.6657_6671del	p.(Arg2220_Pro2224del)		41.5	466		Moderate	Overlap
10	chr16 2,141,910	40	c.11412-3C > A			27.7	20		Low	Overlap
11	chr16 2,167,589	6	c.1286G > T	p.(Trp429Leu)		32.7	313	Probably damaging (0.999)	Moderate	Overlap
11	chr16 2,153,765	23	c.8293C > T	p.(Arg2765Cys)	CM092156 rs144979397	41.1	572	Probably damaging (0.988)	Moderate	Overlap
11	chr16 2,152,396	25	c.9187C > T	p.(Arg3063Cys)	rs145906459	36.1	557	Benign (0.39)	Moderate	Overlap
12	chr16 2,154,643	21	c.8017-2,8017-1del			48.5	527		High	Overlap
13	chr16 2,152,062		c.(287 + 1_288-1)_(9397 + 1_9398-1)del							PacBio
14	chr16 2,141,581	42	c.11554del	p.(Leu3852TrpfsTer93)	rs724159823	41.3	46		High	Overlap
14	chr16 2,162,850	13	c.3100A > G	p.(Asn1034Asp)	rs369180760	36.5	321	Benign (0.098)	Moderate	Overlap
15	chr16 2,158,944	15	c.6223_6224insTT	p.(Arg2075LeufsTer42)		43.3	1,203		High	Sanger
16	chr16 2,164,754	11	c.2269del	p.(Gln757SerfsTer28)	rs775710328	28.4	519		High	Overlap
17	chr16 2,160,198	15	c.4968_4969delinsC	p.(Arg1657GlyfsTer65)		41.2	1,120		High	Overlap
18	chr16 2,157,954	16	c.6994_7000dup	p.(Ala2332GlyfsTer90)		23.4	913		High	Overlap
19	chr16 2,139,750	46	c.12890A > G	p.(Lys4297Arg)	rs758833703	14.1	46	Benign (0.07)	Moderate	PacBio
19	chr16 2,160,919	15	c.4248dup	p.(Gly1417TrpfsTer14)		24.8	979		High	Overlap

Notes: Sanger-detected pathogenic variants are shown in bold. PacBio variants were filtered by coding sequence predicted effects (frameshifts, missense, in-frame deletions, and splicing variants), as well as DP > 15 and > 50 subreads, and variant frequency (> 10% for substitutions, and > 15% for insertions and deletions) (RefSeq NM_001009944.2). Additional information of each variant including SIFT classification, and 1000G frequencies among other annotations can be obtained from the VCF files uploaded to EGA with accession number EGAS00001002106.

analyzing WGS or WES data (Mallawaarachchi et al., 2016; Qi et al., 2013), on the enrichment of *PKD1* using LR-PCR (Rossetti et al., 2012; Tan et al., 2014), or the hybridization capture of *PKD1* (Eisenberger et al., 2015; Trujillano et al., 2014). Two of these studies were performed on short-read NGS using targeted enrichment of *PKD1* or *PKD2* genes by LR-PCR (Rossetti et al., 2012; Tan et al., 2014). In both studies, the use of short reads was the source of difficulties associated with misalignments and lack of sufficient coverage, such as the *PKD1* exon 1 region (Tan et al., 2014), as well as false-positive (10%) and false-negative variant calls (5%) (Rossetti et al., 2012). We show that these challenges were mitigated with long-read sequencing that provided 100% coverage $>10\times$ (minimum $>19\times$; average $>421\times$; maximum 1,528 \times) for all *PKD1* and *PKD2* exons and flanking intron regions (± 20 bp) (Supp. Tables S2 and S4), including 100% of *PKD1* exon 1 at average coverage of $>55\times$ (± 20 bp of flanking intron regions included) (Supp. Table S4). Other WES-based strategies were reported to resolve only 50% of true-positive variants in the duplicated regions of *PKD1* (Qi et al., 2013). It was argued that increasing the sequencing depth was insufficient to overcome the limitations and pitfalls of short-read NGS approaches (Eisenberger et al., 2015; Qi et al., 2013). Similar to these short-read NGS strategies (Eisenberger et al., 2015; Mallawaarachchi et al., 2016; Qi et al., 2013; Rossetti et al., 2012; Tan et al., 2014; Trujillano et al., 2014), our targeted approach combined with multiplexed sequencing can further accelerate ADPKD diagnostics, compared with the labor-intensive Sanger sequencing (Rossetti et al., 2012; Tan et al., 2014). Despite the rather limited sample size, sufficient numbers were included in this study for a methodology evaluation. However, future studies including larger cohorts would be needed to reliably implement the proposed methodology into the clinic. In addition, our method can benefit from recent advancements in library preparation methods with minimal or no amplification, such as single-strand adaptor ligation (Karlsson et al., 2015), which would eliminate most of the biases introduced during LR-PCR amplification steps (Hestand, Houdt, Cristofoli, & Vermeesch, 2016; Laver et al., 2016; Schirmer et al., 2015). Overall, our method provides high sensitivity in identifying *PKD1* genetic variants when compared with the standard ADPKD diagnostic assay and showed an added value to become a reliable alternative. In addition, the method presented here is comparable to other Illumina short-read NGS-based approaches. However, further studies including a larger cohort may be required to decipher the true diagnostic power of our approach compared with that of standard ADPKD diagnostic assays using Sanger and MLPA, and to Illumina short-read NGS-based methods.

In conclusion, we showed that direct sequencing of LR-PCR fragments for the screening of ADPKD patients in a single diagnostic test application is now possible. Accurate screening of *PKD1* with high sensitivity and low interference of homologous sequences constitutes a clear example. This method is highly valuable for a diagnostic setting, as it increases the resolution power of clinically relevant but difficult to sequence or to resolve genomic regions.

ACKNOWLEDGMENTS

This study was performed within the scope of the iMODE-CKD Initial Training Network (ITN) (Clinical and system-omics for the

identification of the Molecular Determinants of established Chronic Kidney Disease).

Data obtained from Rossetti et al. (2012) was kindly provided by Peter C. Harris and Christina M. Heyer (Mayo Clinic College of Medicine).

Patient samples were kindly provided by the DIPAK Consortium, an interuniversity collaboration in The Netherlands, established to study ADPKD and to develop rational treatment strategies for this disease (www.nierstichting.nl/dipak). Principal investigators are (in alphabetical order): J. P. H. Drenth (Department of Gastroenterology and Hepatology, Radboud University Medical Center Nijmegen), J. W. de Fijter (Department of Nephrology, Leiden University Medical Center), R. T. Gansevoort (Department of Nephrology, University Medical Center Groningen), D. J. M. Peters (Department of Human Genetics, Leiden University Medical Center), J. Wetzels (Department of Nephrology, Radboud University Medical Center Nijmegen), and R. Zietse (Department of Internal Medicine, Erasmus Medical Center Rotterdam).

We acknowledge the continued support of Joost P. Schanstra (Inserm; Université Toulouse III Paul Sabatier, Institut de Médecine Moléculaire de Rangueil).

DISCLOSURE STATEMENT

The authors declare no conflict of interest.

REFERENCES

- Barua, M., Cil, O., Paterson, A. D., Wang, K., He, N., Dicks, E., ... Pei, Y. (2009). Family history of renal disease severity predicts the mutated gene in ADPKD. *Journal of the American Society of Nephrology*, 20, 1833–1838.
- Chaisson, M. J., & Tesler, G. (2012). Mapping single molecule sequencing reads using basic local alignment with successive refinement (BLASR): Application and theory. *BMC Bioinformatics*, 13, 238.
- Chaisson, M. J. P., Huddleston, J., Dennis, M. Y., Sudmant, P. H., Malig, M., Hormozdiari, F., ... Stamatoyannopoulos, J. A. (2015). Resolving the complexity of the human genome using single-molecule sequencing. *Nature*, 517, 608–611.
- Chang, F., & Li, M. M. (2013). Clinical application of amplicon-based next-generation sequencing in cancer. *Cancer Genetics*, 206, 413–419.
- Codina-Solà, M., Rodríguez-Santiago, B., Homs, A., Santoyo, J., Rigau, M., Aznar-Laín, G., ... Antiñolo, G. (2015). Integrated analysis of whole-exome sequencing and transcriptome profiling in males with autism spectrum disorders. *Molecular Autism*, 6, 21.
- den Dunnen, J. T., Dalgleish, R., Maglott, D. R., Hart, R. K., Greenblatt, M. S., McGowan-Jordan, J., ... Taschner, P. E. M. (2016). HGVS recommendations for the description of sequence variants: 2016 update. *Human Mutation*, 37, 564–569.
- de Ligt, J., Willemsen, M. H., van Bon, B. W. M., Kleefstra, T., Yntema, H. G., Kroes, T., ... Hoischen, A. (2012). Diagnostic exome sequencing in persons with severe intellectual disability. *The New England Journal of Medicine*, 367, 1921–1929.
- Dewey, F. E., Grove, M. E., Pan, C., Goldstein, B. A., Bernstein, J. A., Chaib, H., ... Ormond, K. E. (2014). Clinical interpretation and implications of whole-genome sequencing. *JAMA*, 311, 1035.
- Eisenberger, T., Decker, C., Hiersche, M., Hamann, R. C., Decker, E., Neuber, S., ... Mache, C. (2015). An efficient and comprehensive strategy for genetic diagnostics of polycystic kidney disease. *PLoS One*, 10, e0116680.

- Gout, A. M., Martin, N. C., Brown, A. F., & Ravine, D. (2007). PKDB: Polycystic kidney disease mutation database—A gene variant database for autosomal dominant polycystic kidney disease. *Human Mutation*, 28, 654–659.
- Guo, X., Zheng, S., Dang, H., Pace, R. G., Stonebraker, J. R., Jones, C. D., ... Seibold, M. A. (2013). Genome reference and sequence variation in the large repetitive central exon of human muc5ac. *American Journal of Respiratory Cell and Molecular Biology*, 50, 223–232.
- Harris, P. C., & Rossetti, S. (2010). Molecular diagnostics for autosomal dominant polycystic kidney disease. *Nature Reviews Nephrology*, 6, 197–206.
- Hestand, M. S., Houdt, J. V., Cristofoli, F., & Vermeesch, J. R. (2016). Polymerase specific error rates and profiles identified by single molecule sequencing. *Mutation Research/Fundamental and Molecular Mechanisms of Mutagenesis*, 784–785, 39–45.
- Karlsson, K., Sahlin, E., Iwarsson, E., Westgren, M., Nordenskjöld, M., & Linnarsson, S. (2015). Amplification-free sequencing of cell-free DNA for prenatal non-invasive diagnosis of chromosomal aberrations. *Genomics*, 105, 150–158.
- LaDuca, H., Stuenkel, A. J., Dolinsky, J. S., Keiles, S., Tandy, S., Pesaran, T., ... Speare, V. (2014). Utilization of multigene panels in hereditary cancer predisposition testing: Analysis of more than 2,000 patients. *Genetics Medicine*, 16, 830–837.
- Laver, T. W., Caswell, R. C., Moore, K. A., Poschmann, J., Johnson, M. B., Owens, M. M., ... Weedon, M. N. (2016). Pitfalls of haplotype phasing from amplicon-based long-read sequencing. *Scientific Reports*, 6, 21746.
- Lee, H., & Schatz, M. C. (2012). Genomic dark matter: The reliability of short read mapping illustrated by the genome mappability score. *Bioinformatics*, 28, 2097–2105.
- Loomis, E. W., Eid, J. S., Peluso, P., Yin, J., Hickey, L., Rank, D., ... Hagerman, P. J. (2013). Sequencing the unsequenceable: Expanded CGG-repeat alleles of the fragile X gene. *Genome Research*, 23, 121–128.
- Mallawaarachchi, A. C., Hort, Y., Cowley, M. J., McCabe, M. J., Minoche, A., Dinger, M. E., ... Furlong, T. J. (2016). Whole-genome sequencing overcomes pseudogene homology to diagnose autosomal dominant polycystic kidney disease. *European Journal of Human Genetics*, 24, 1584–1590.
- Mardis, E. R. (2013). Next-Generation sequencing platforms. *Annual Review of Analytical Chemistry*, 6, 287–303.
- McLaren, W., Pritchard, B., Rios, D., Chen, Y., Flicek, P., & Cunningham, F. (2010). Deriving the consequences of genomic variants with the Ensembl API and SNP Effect Predictor. *Bioinformatics*, 26, 2069–2070.
- Oliver, G. R., Hart, S. N., & Klee, E. W. (2015). Bioinformatics for clinical next generation sequencing. *Clinical Chemistry*, 61, 124–135.
- Ozsolak, F., & Milos, P. M. (2011). Single-molecule direct RNA sequencing without cDNA synthesis. *Wiley Interdisciplinary Reviews: RNA*, 2, 565–570.
- Qi, X.-P., Du, Z.-F., Ma, J.-M., Chen, X.-L., Zhang, Q., Fei, J., ... Chen, Z.-G. (2013). Genetic diagnosis of autosomal dominant polycystic kidney disease by targeted capture and next-generation sequencing: Utility and limitations. *Gene*, 516, 93–100.
- Qiao, W., Yang, Y., Sebra, R., Mendiratta, G., Gaedigk, A., Desnick, R. J., & Scott, S. A. (2016). Long-read single molecule real-time full gene sequencing of cytochrome P450-2D6: Human mutation. *Human Mutation*, 37, 315–323.
- Rossetti, S., Consugar, M. B., Chapman, A. B., Torres, V. E., Guay-Woodford, L. M., Grantham, J. J., ... Thompson, P. A. (2007). Comprehensive molecular diagnostics in autosomal dominant polycystic kidney disease. *Journal of the American Society Nephrology*, 18, 2143–2160.
- Rossetti, S., Hopp, K., Sikkink, R. A., Sundsbak, J. L., Lee, Y. K., Kubly, V., ... Harris, P. C. (2012). Identification of gene mutations in autosomal dominant polycystic kidney disease through targeted resequencing. *Journal of the American Society of Nephrology*, 23, 915–933.
- Schirmer, M., Ijaz, U. Z., D'Amore, R., Hall, N., Sloan, W. T., & Quince, C. (2015). Insight into biases and sequencing errors for amplicon sequencing with the Illumina MiSeq platform. *Nucleic Acids Research*, 43, e37–e37.
- Spithoven, E. M., Kramer, A., Meijer, E., Orskov, B., Wanner, C., Abad, J. M., ... Heaf, J. (2014). Renal replacement therapy for autosomal dominant polycystic kidney disease (ADPKD) in Europe: Prevalence and survival—An analysis of data from the ERA-EDTA Registry. *Nephrology Dialysis Transplantation*, 29, iv15–iv25.
- Steinberg, K. M., Schneider, V. A., Graves-Lindsay, T. A., Fulton, R. S., Agarwala, R., Huddleston, J., ... Eichler, E. E. (2014). Single haplotype assembly of the human genome from a hydatidiform mole. *Genome Research*, 24, 2066–2076.
- Su, Z., Ning, B., Fang, H., Hong, H., Perkins, R., Tong, W., Shi, L. (2011). Next-generation sequencing and its applications in molecular diagnostics. *Expert Review of Molecular Diagnosis*, 11, 333–343.
- Sun, Y., Ruivenkamp, C. A. L., Hoffer, M. J. V., Vrijenhoek, T., Kriek, M., van Asperen, C. J., ... Santen, G. W. E. (2015). Next-generation diagnostics: Gene panel, exome, or whole genome? *Human Mutation*, 36, 648–655.
- Tan, A. Y., Michael, A., Liu, G., Elemento, O., Blumenfeld, J., Donahue, S., ... Rennert, H. (2014). Molecular diagnosis of autosomal dominant polycystic kidney disease using next-generation sequencing. *The Journal of Molecular Diagnostics*, 16, 216–228.
- Tan, Y.-C., Blumenfeld, J. D., Anghel, R., Donahue, S., Belenkaya, R., Balina, M., ... Rennert, H. (2009). Novel method for genomic analysis of PKD1 and PKD2 mutations in autosomal dominant polycystic kidney disease. *Human Mutation*, 30, 264–273.
- Trujillano, D., Bullich, G., Ossowski, S., Ballarín, J., Torra, R., Estivill, X., & Ars, E. (2014). Diagnosis of autosomal dominant polycystic kidney disease using efficient PKD1 and PKD2 targeted next-generation sequencing. *Molecular Genetics Genomic Medicine*, 2, 412–421.
- Vis, J. K., Vermaat, M., Taschner, P. E. M., Kok, J. N., & Laros, J. F. J. (2015). An efficient algorithm for the extraction of HGVS variant descriptions from sequences. *Bioinformatics*, 31, 3751–3757.
- von Kanel, T., & Huber, A. R. (2013). DNA methylation analysis. *Swiss Medical Weekly*, 143, w13799.
- Wildeman, M., van Ophuizen, E., den Dunnen, J. T., & Taschner, P. E. M. (2008). Improving sequence variant descriptions in mutation databases and literature using the Mutalyzer sequence variation nomenclature checker. *Human Mutation*, 29, 6–13.
- Willig, L. K., Petrikin, J. E., Smith, L. D., Saunders, C. J., Thiffault, I., Miller, N. A., ... Kingsmore, S. F. (2015). Whole-genome sequencing for identification of Mendelian disorders in critically ill infants: A retrospective analysis of diagnostic and clinical findings. *The Lancet Respiratory Medicine*, 3, 377–387.
- Yang, Y., Muzny, D. M., Reid, J. G., Bainbridge, M. N., Willis, A., Ward, P. A., ... Eng, C. M. (2013). Clinical whole-exome sequencing for the diagnosis of Mendelian disorders. *The New England Journal of Medicine*, 369, 1502–1511.

SUPPORTING INFORMATION

Additional Supporting Information may be found online in the supporting information tab for this article.

How to cite this article: Borràs DM, Vossen R, Liem M, et al. Detecting PKD1 variants in polycystic kidney disease patients by single-molecule long-read sequencing. *Human Mutation*. 2017;38:870–879. <https://doi.org/10.1002/humu.23223>